



Carbazole-Fused Coumarin Bis Oxime Esters (CCOBOEs) as efficient photoinitiators of polymerization for 3D printing with 405 nm LED

Zheng Liu, Tong Gao, Yijun Zhang, Céline Dietlin, Fabrice Morlet-Savary,
Michael Schmitt, Dider Gigmes, Frédéric Dumur, Jacques Lalevée

► To cite this version:

Zheng Liu, Tong Gao, Yijun Zhang, Céline Dietlin, Fabrice Morlet-Savary, et al.. Carbazole-Fused Coumarin Bis Oxime Esters (CCOBOEs) as efficient photoinitiators of polymerization for 3D printing with 405 nm LED. European Polymer Journal, 2024, pp.113186. 10.1016/j.eurpolymj.2024.113186 . hal-04614944

HAL Id: hal-04614944

<https://hal.science/hal-04614944>

Submitted on 17 Jun 2024

HAL is a multi-disciplinary open access archive for the deposit and dissemination of scientific research documents, whether they are published or not. The documents may come from teaching and research institutions in France or abroad, or from public or private research centers.

L'archive ouverte pluridisciplinaire **HAL**, est destinée au dépôt et à la diffusion de documents scientifiques de niveau recherche, publiés ou non, émanant des établissements d'enseignement et de recherche français ou étrangers, des laboratoires publics ou privés.

Carbazole-Fused Coumarin Bis Oxime Esters (CCOBOEs) as efficient photoinitiators of polymerization for 3D printing with 405 nm LED

Zheng Liu¹, Tong Gao², Yijun Zhang², Céline Dietlin², Fabrice Morlet-Savary², Michael Schmitt², Didier Gigmes¹, Frédéric Dumur^{*1} and Jacques Lalevée^{*2}

¹Aix Marseille Univ, CNRS, ICR UMR 7273, F-13397 Marseille, France

²Université de Haute-Alsace, CNRS, IS2M UMR 7361, F-68100 Mulhouse, France

*Corresponding authors: frederic.dumur@univ-amu.fr; jacques.lalevee@uha.fr

Abstract

In this research, the innovative design and successful synthesis of two visible light photoinitiators, namely CCOBOE0 and CCOBOE1, have been confirmed through nuclear magnetic resonance (NMR) and mass spectrometry (MS). Both compounds exhibit strong absorption properties at 385, 405 and 450 nm, and FT-IR analyses have substantiated the ability of CCOBOE1 to initiate the polymerization of a trifunctional acrylate monomer (TMPTA) under these three light sources. The optimal conditions for maximizing the photoinitiation potential of CCOBOE1 were determined to be at a concentration of 2×10^{-5} mol.g⁻¹ and under 405 nm LED irradiation. Photolysis experiments, theoretical calculations, detection of CO₂ absorption peaks, and ESR experiments have all confirmed the generation of methyl radicals by CCOBOE1. Utilizing the identified optimal conditions, a "XYZ" pattern with a thickness of 963 μm and a 3D-object were successfully obtained *via* direct laser write (DLW) and digital light processing (DLP) 3D-printing upon irradiation at 405 nm. Additionally, differential scanning calorimetry (DSC) analyses demonstrated the promising performance of CCOBOE1 in initiating the thermal polymerization of acrylate monomers. In summary, the difunctional CCOBOE1 showed outstanding performance in both photo-initiation and thermal initiation of acrylate monomers. It provides a novel direction for the development of novel OXEs with dual activation modes.

1. Introduction

In recent years, the development of highly efficient photoinitiators for polymerization processes done under mild conditions has garnered a significant attention in the fields of photochemistry and polymer science.^[1-3] Among all photoinitiators reported in the literature, oxime esters (OXEs) are interesting structures as these photoinitiators can act as monocomponent photoinitiating systems. The oxime group can be easily connected to various chromophores, so that oxime esters are promising candidates for the future development of visible light photopolymerization due to the facile tunability of the absorption properties by mean of a careful selection of the chromophore, but also the reactivity of OXEs thanks to the group which is used to esterify the oxime group.^[4-6] Notably, recent works have clearly demonstrated the higher reactivity of OXEs bearing aliphatic groups on the ester side compared to the aromatic analogues.^[7, 8] With aim at developing cheap and easily accessible photoinitiators, OXEs can typically be prepared in three steps using cheap reagents such as sodium acetate, hydroxylamine hydrochloride or triethylamine, so that the future use of these photoinitiators in industry is almost ensured. To end, a great deal of efforts has been devoted during the last three years by academics to develop visible light OXEs. With aim at identifying the most reactive chromophore, a series of dyes have been screened, as exemplified by triphenylamines^[9-12], naphthalenes^[13], coumarins^[14, 15], anthraquinones^[16], phenylthioether thiophenes^[17, 18], fluorophenyl derivatives^[19], stilbene derivatives^[20], thiophene derivatives^[21], naphthalimides^[22] or naphthoquinones^[23].

The hybrid chromophore formed by the partial fusion of a carbazole (nitrogen-containing five-membered heterocycle) and a coumarin (benzopyranone derivative) represents a novel class of compounds with distinctive photoresponsive characteristics.^[24, 25] This unique structure arises from the fusion of two different aromatic systems, creating a new π -conjugated system with synergistic properties that leverage the complementary features of both components. It encompasses the electron-rich nature of carbazole, along with the excellent light absorption and fluorescence properties of coumarin.^[5, 6, 26, 27] Therefore, the fused chromophore, with its unique electronic structure, exhibits absorption properties and a photochemical reactivity

which is different from that of the two chromophores considered separately.^[25,28,29] The potential of these carbazole-coumarin hybrid dyes for promoting intramolecular electron transfer and energy transfer processes makes these structures highly suitable candidates for applications in photopolymerization.

To date, use of carbazole-coumarin hybrid dyes as chromophores for the design of oxime esters has been reported only twice in the literature. In 2020, Zhou et al. pioneered the design and synthesis of four new oxime ester photoinitiators incorporating carbazole, coumarin, and oxime ester functionalities, and exhibiting maximum absorption peaks around 374 nm.^[30] By use of four different light sources (365, 385, 405, and 425 nm) for 200 s, the four OXEs demonstrated excellent polymerization kinetics during the free radical polymerization of a trifunctional monomer, namely trimethylolpropane triacrylate (TMPTA), although the maximum conversion rates didn't exceed 50% at a concentration of 1 wt% in TMPTA under air using a photo-DSC instrument.

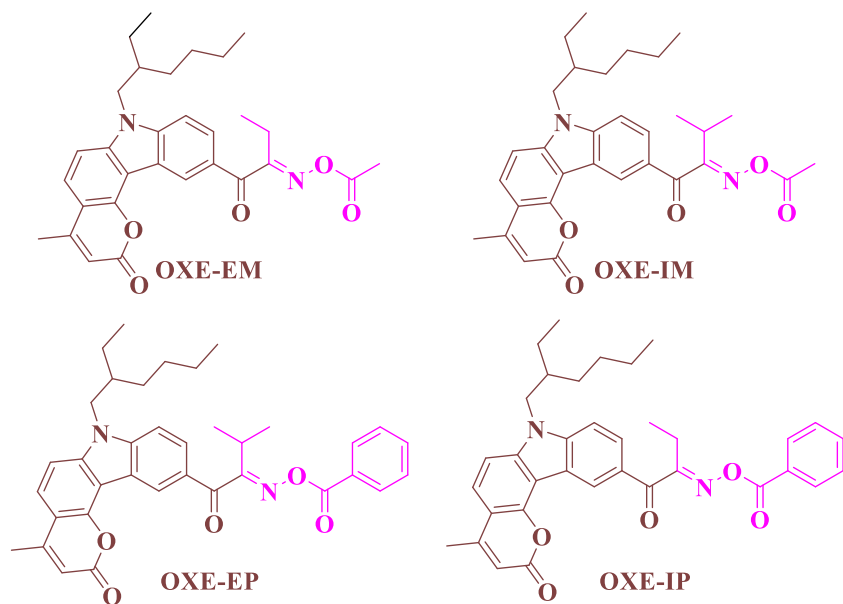


Figure 1. Structures of the four reported coumarin-fused carbazole OXEs.

In 2023, to enhance the photopolymerization efficiency of the carbazole-coumarin hybrid oxime esters, Zhang et al. prepared a series of 16 novel OXEs with absorption maxima around 378-383 nm.^[31] Theoretical calculations revealed the photocleavage of these OXEs to be more favorable from the singlet excited state than from the triplet state upon excitation at 405 nm. Among the 16 structures investigated, OXE-1 (65%),

OXE-5 (68%), and OXE-7 (65%) could outperform the commercial diphenyl(2,4,6-trimethylbenzoyl)phosphine oxide (TPO) (63%) at a concentration of 2×10^{-5} mol.g⁻¹ in TMPTA under laminate with the thickness at 25 μm.

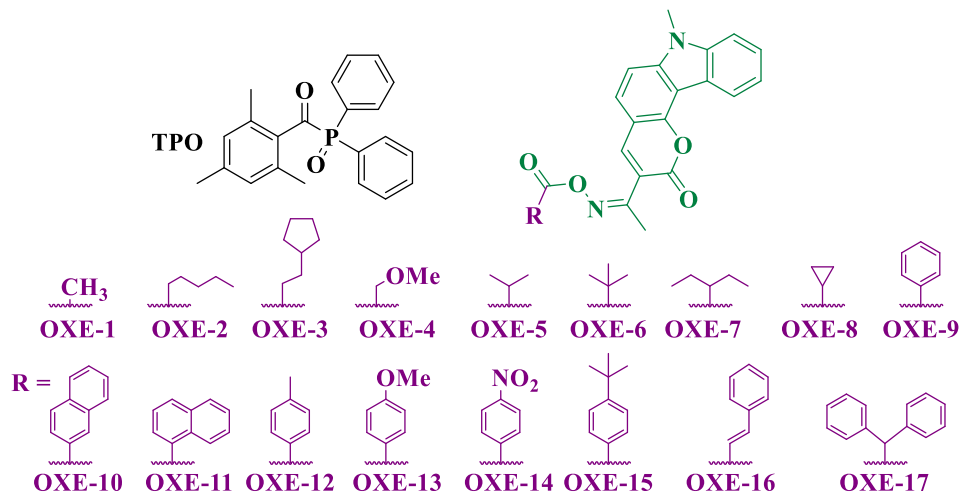


Figure 2. Structures of the TPO and 16 reported carbazole-coumarin hybrid oxime esters

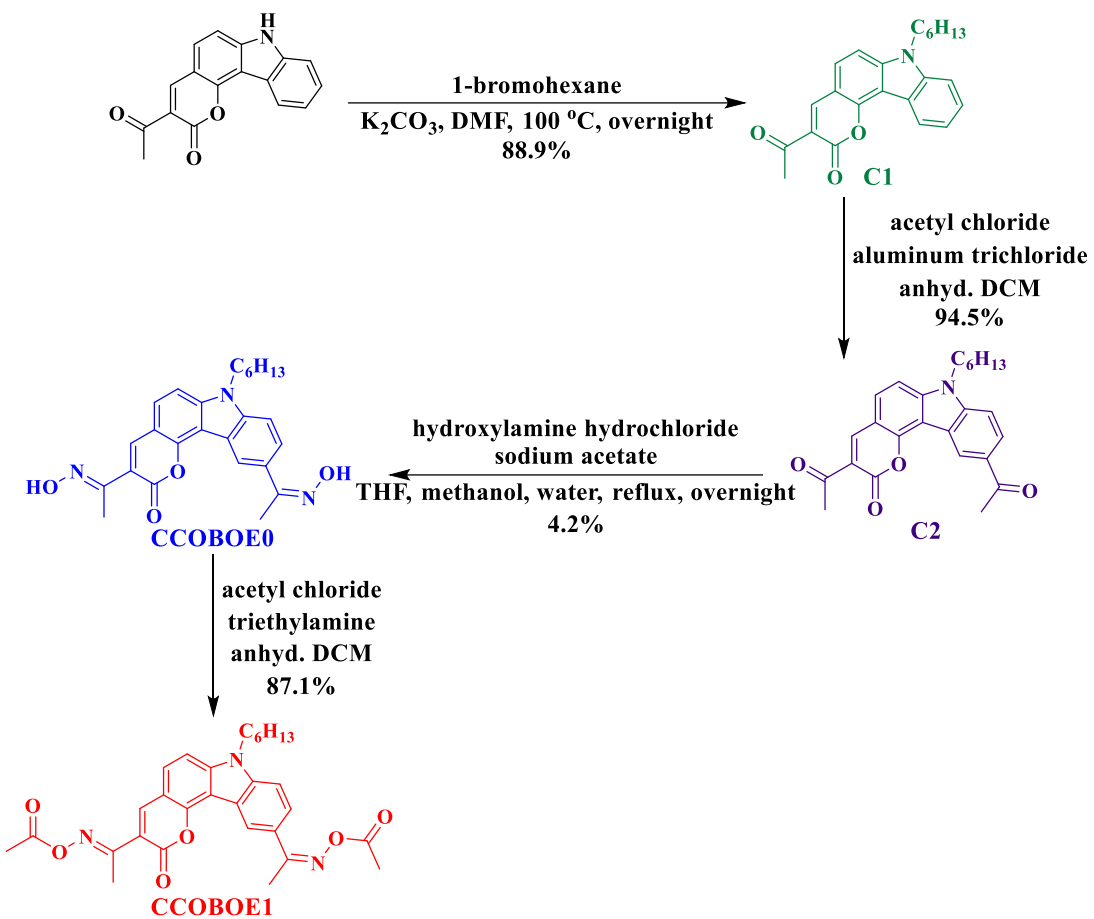
Numerous factors influence the polymerization kinetics of Type I photoinitiators, such as the intramolecular charge transfer efficiency, the radical reactivity after cleavage, photocleavage from the singlet or the triplet excited state energies, the N-O bond dissociation energy (BDE) of OXE, and the excited state lifetime.^[2-4, 32] However, examination of the influence of the number of oxime ester groups per molecule on the polymerization efficiency is rarely examined. This study is thus devoted to investigate the reactivity of a difunctional carbazole-coumarin hybrid OXE, namely CCOBOE1 and its potential application in photoinduced polymerization. For comparison, a monofunctional carbazole-coumarin hybrid OXE i.e. OXE-1 was used (see Figure 2).^[31] Chemical structure of CCOBOE1 was confirmed by nuclear magnetic resonance (NMR) spectroscopy and high-resolution mass spectrometry (HRMS). Absorption and photodecomposition properties of CCOBOEs were obtained by UV-visible absorption spectroscopy of the compounds dissolved in dichloromethane (DCM). Singlet and triplet state energies as well as the BDE of the N-O bond were determined using the crossing point of the normalized absorption and emission curves and by theoretical calculations, respectively. A photopolymerization mechanism involving CCOBOE1 as the photoinitiator was proposed and confirmation of the photocleavage followed by a

decarboxylation reaction was evidenced by the detection of a CO₂ absorption peak by Fourier-transform infrared spectroscopy (FT-IR) during the polymerization process. Three different light sources and two different concentrations of CCOBOEs in TMPTA were used to investigate the influence of the light sources and the concentrations on the polymerization kinetics. The optimized photo-polymerization conditions were employed to 3D print a predefined pattern through direct laser writing (DLW). Additionally, Differential Scanning Calorimetry (DSC) was employed to assess the thermal polymerization characteristics of the CCOBOE/TMPTA systems.

2. Results and discussion

2.1 Synthesis of the dyes

The synthetic procedure used to prepare 3-acetylpyrano[3,2-*c*]carbazol-2(7*H*)-one has been reported in a previous study.^[31] Starting from 3-acetyl-7-hexylpyrano[3,2-*c*]pyrazole as the initial material, alkylation of the NH group of carbazole with 1-bromohexane in the presence of K₂CO₃ as the base furnished the compound C1 with a yield of 88.9%. Subsequently, an acylation reaction was employed to introduce an additional acetyl group on the scaffold, affording compound C2 with a yield of 94.5%. Following this, a condensation reaction of hydroxylamine hydrochloride on the carbonyl group using sodium acetate as the base formed CCOBOE0 as a bifunctional oxime ester. However, due to the high reactivity of the lactone moiety towards hydroxylamine and a ring-opening reaction, the reaction yield for this step was limited to 4.2%. Finally, CCOBOE1 was obtained through a classical esterification of the oxime group with acetyl chloride in the presence of triethylamine, providing the targeted compound in 87.1% yield.



Scheme 1. Synthetic routes to CCOBOEs

2.2 Light absorption properties

Figure 3 shows the UV-visible absorption spectra of CCOBOE0 and CCOBOE1 dissolved in dichloromethane (DCM). Table 1 provides details concerning their maximum absorption wavelengths (λ_{\max}) and molar extinction coefficients (ϵ) at λ_{\max} , 405 nm and 450 nm. CCOBOEs exhibit favorable solubility in DCM. As depicted in Figure 3, CCOBOE0 and CCOBOE1, with λ_{\max} at 380 nm and 385 nm respectively, both exhibit a broad absorption band extending up to 500 nm. Compared to CCOBOE0, esterification of the oxime groups in CCOBOE1 only resulted in a subtle redshift of the λ_{\max} of CCOBOE1 by ca. 5 nm. This is directly related to the fact that the two oxime ester groups are not involved in the π -conjugated system of the carbazole-coumarin hybrid structure and thus can be considered as simple side-groups connected to the carbazole-coumarin core. Parallel to this, a slight enhancement of the ϵ_{\max} of

CCOBOE1 is also detected, reaching $14100 \text{ M}^{-1}.\text{cm}^{-1}$. Meanwhile, the $\epsilon_{405 \text{ nm}}$ of CCOBOE1 is $10000 \text{ M}^{-1}.\text{cm}^{-1}$, surpassing CCOBOE0, which is measured at $8000 \text{ M}^{-1}.\text{cm}^{-1}$. Unfortunately, $\epsilon_{450 \text{ nm}}$ of CCOBOE0 is the same that of CCOBOE1, measuring $800 \text{ M}^{-1}.\text{cm}^{-1}$. In summary, both CCOBOE0 and CCOBOE1 demonstrate notable absorption characteristics at 385, 405 and 450 nm, establishing them as suitable candidates for photoinitiation at these three wavelengths.

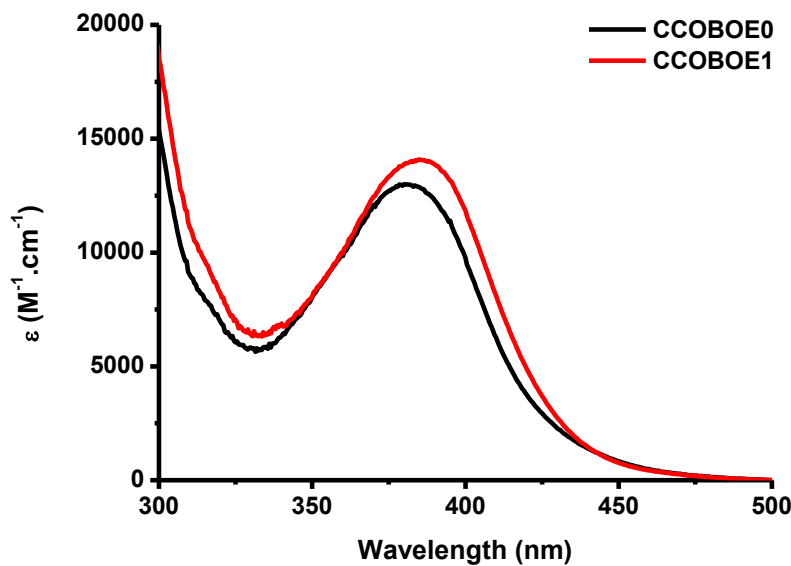


Figure 3. UV-vis absorption spectra of CCOBOEs (concentration: $2 \times 10^{-5} \text{ M}$) in DCM

Table 1. Light absorption properties of CCOBOEs

CCOBOEs	λ_{\max} (nm)	ϵ_{\max} ($\text{M}^{-1}.\text{cm}^{-1}$)	$\epsilon_{405 \text{ nm}}$ ($\text{M}^{-1}.\text{cm}^{-1}$)	$\epsilon_{450 \text{ nm}}$ ($\text{M}^{-1}.\text{cm}^{-1}$)
CCOBOE0	380	13000	8000	800
CCOBOE1	385	14100	10000	800

2.3 Steady-state photolysis

To investigate the photoreactivity of CCOBOEs, the two compounds were dissolved in DCM and photolysis experiments were carried out at three different wavelengths i.e. 385, 405 and 450 nm at a concentration of $2 \times 10^{-5} \text{ M}$. The absorption intensities in the 300-500 nm range were measured using a UV-vis spectrophotometer after 0, 5, 10, 20, 30, 40, 50 and 60 s of irradiation (See Figure 4).

As shown in Figure 4, under 385 nm LED irradiation, both CCOBOE0 and CCOBOE1

exhibited a decrease of the absorbance upon irradiation. However, compared to CCOBOE0, the decrease of absorbance is significantly more pronounced for CCOBOE1. Surprisingly, after 10 s of irradiation with a 405 nm LED, CCOBOE0 showed an increase of its absorbance, and the upward trend is nearly stagnant thereafter. Reproducibility of this unexpected behavior has been verified by repeating the photolysis experiments. Clearly, a reproducible behavior of absorbance increase could be evidenced which can be tentatively assigned to the formation of a photoproduct at this specific wavelength. Besides, this behavior could not be more rationalized. In contrast, CCOBOE1 consistently experiences a gradual decrease of absorbance upon irradiation at 405 nm, with a photolysis pattern similar to that observed at 385 nm. Since both CCOBOE0 and CCOBOE1 have low absorbance at 450 nm, their low photochemical reactivities can thus be anticipated at this wavelength. Consequently, the change in absorbance after 450 nm irradiation is minimal for CCOBOE0, while the absorbance intensity of CCOBOE1, although decreasing with increasing the irradiation time, exhibits a much lower reduction compared to that detected at the two other wavelengths. In conclusion, it is gratifying to observe that CCOBOE1 undergoes noticeable photolysis under 385, 405, and 450 nm LED irradiation, indicating the cleavage of its oxime ester functionality, making it suitable for excitation under these three light sources to initiate the free radical polymerization of acrylate monomers.

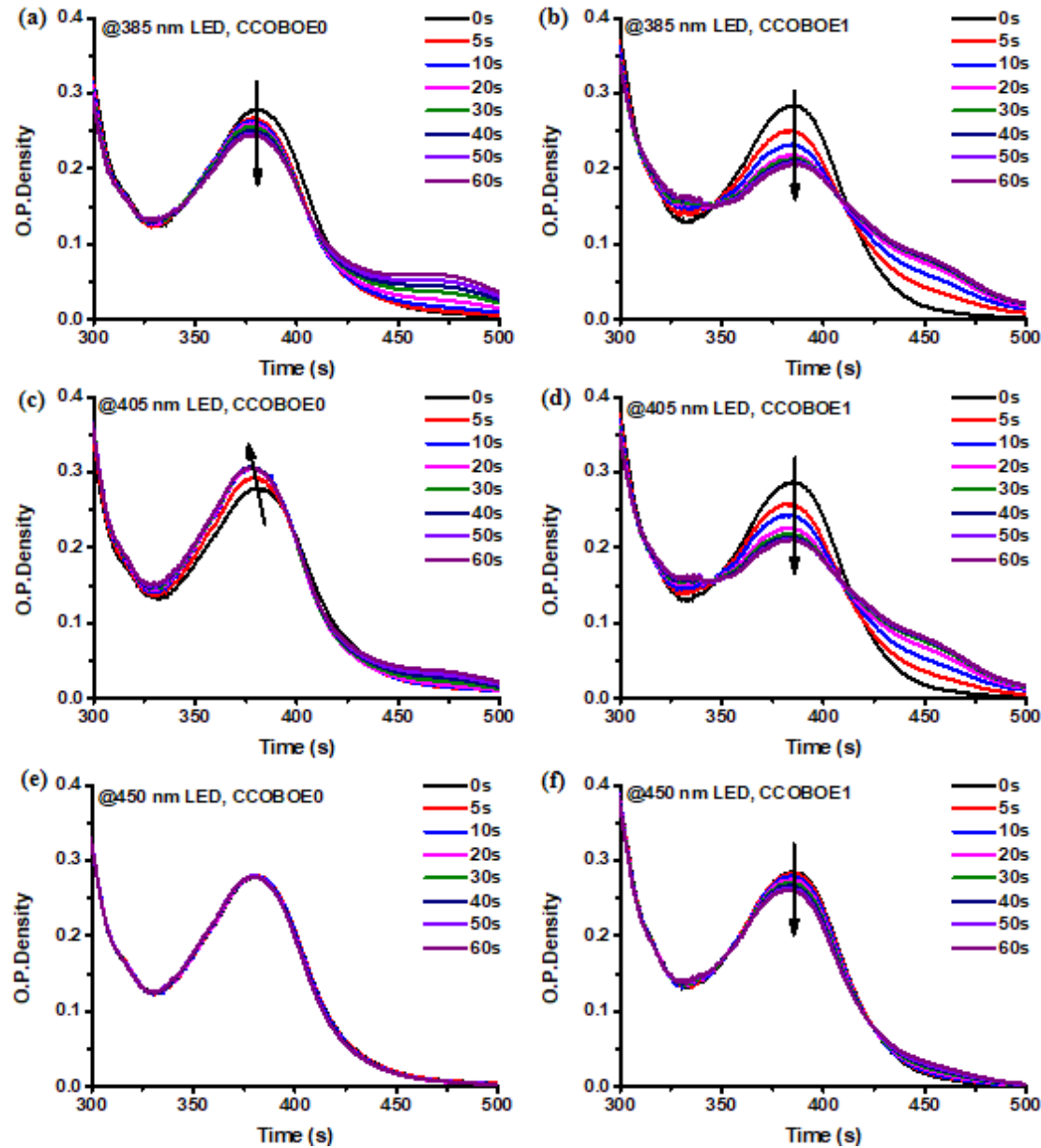


Figure 4. Steady-state photolysis of CCOBOE0 and CCOBOE1 in DCM (concentration: 2×10^{-5} M) upon irradiation with 385 nm (a, b), 405 nm (c, d), 450 nm (e, f) LEDs

2.4 Free radical photopolymerization

To comprehensively analyze the impact of the CCOBOEs concentrations and the different light sources on the photoinitiating ability of these structures during the FRP of TMPTA, these two points were investigated in detail. Figure 5 and S1 shows the polymerization curves obtained with CCOBOEs at two different concentrations (5×10^{-6} mol.g⁻¹ and 2×10^{-5} mol.g⁻¹) and for three different irradiation wavelengths (385, 405,

and 450 nm). Table 2 provides a summary of the final monomer conversions (FCs) obtained under these different conditions. Firstly, as shown in Figure S1, it is noteworthy that CCOBOE0 failed to initiate the polymerization of TMPTA irrespective of the conditions (concentration, irradiation wavelength or irradiation time) and attributed to the absence of photocleavable groups in CCOBOE0. Indeed, CCOBOE0 is not an oxime ester but only an oxime which is not capable to fragment upon photoexcitation. By itself, this structure is unable to produce any radicals without additives.

As shown in Figure 5, increase of the concentration of CCOBOE1 positively influenced the polymerization of TMPTA under 385 nm and 405 nm LED irradiation but had an adverse effect under 450 nm LED irradiation. This trend of reactivity perfectly coincides with the absorption characteristics of CCOBOE1. Indeed, CCOBOE1 exhibits a strong absorption at 385 and 405 nm but only a weak absorption at 450 nm. By increasing the concentration, the light penetration within the resins is hindered (inner filter effect), leading to a low cleavage efficiency. Parallel to this, by increasing the photoinitiator concentration in resins, a bad solubility can occur, adversely affecting the monomer conversion. This effect can be strengthened by using a less-energetic irradiation wavelength, as observed in our case at 450 nm. By comparing the different data, the optimal conditions for the CCOBOE1/TMPTA system were identified as being 2×10^{-5} mol.g⁻¹ and the most appropriate irradiation wavelength to be 405 nm. Under these conditions, CCOBOE1 demonstrated a superior cleavage efficiency, resulting in a higher production of methyl radicals, so that the FC could reach 70% after 300 s of irradiation. Compared to the monofunctional coumarin-fused carbazole oxime ester OXE-1, which contains a single oxime ester group (FC = 65%) [31], CCOBOE1 exhibits a stronger initiating effect at the same concentration under 405 nm LED irradiation. This indicates that the introduction of the bis-oxime ester group enhances the photoinitiation efficiency.

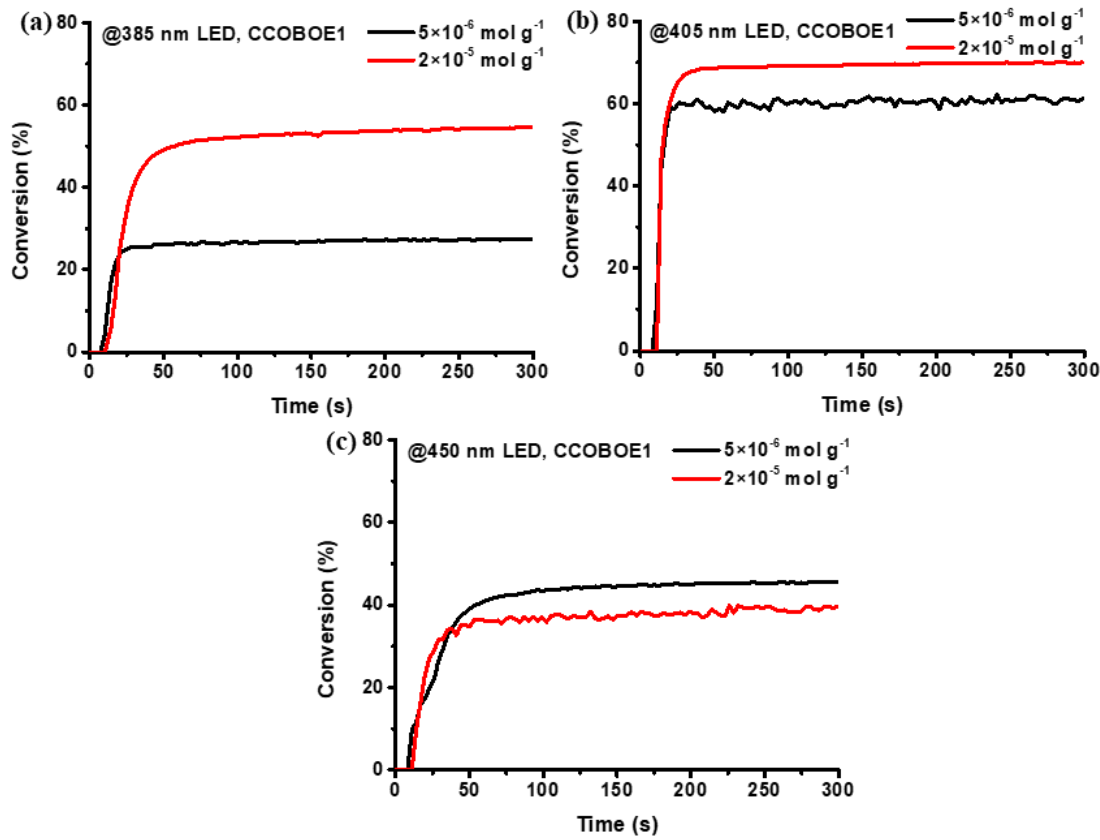


Figure 5. Photopolymerization profiles of TMPTA in laminate (25 μm) upon exposure to a 385 nm (a), 405 nm (b) and 450 nm (c) LED in the presence of CCOBOE1 ($5 \times 10^{-6} \text{ mol.g}^{-1}$ and $2 \times 10^{-5} \text{ mol.g}^{-1}$ in TMPTA). The irradiation starts at $t = 10 \text{ s}$

Table 2. Final acrylate function conversions (FCs) of TMPTA containing different CCOBOEs

Light sources	FCs (%)			
	$5 \times 10^{-6} \text{ mol.g}^{-1}$		$2 \times 10^{-5} \text{ mol.g}^{-1}$	
	CCOBOE0	CCOBOE1	CCOBOE0	CCOBOE1
385 nm LED	< 5%	28	< 5%	55
405 nm LED	< 5%	61	< 5%	70
450 nm LED	< 5%	46	< 5%	40

2.5 The decarboxylation reaction

To theoretically explain the easy cleavage of the N-O bond in CCOBOEs, Figure S2(a,

b) illustrates the normalized curves of the UV-vis absorption spectra and fluorescence spectra of CCOBOE0 and CCOBOE1. Energy levels of the singlet excited states (E_{S1}) were determined by calculating the abscissa of their intersection points. Conversely, the N-O BDE, and E_T were determined by theoretical calculations, as presented in Table 3. Figures S2(c, d) depict the fluorescence decay curves of CCOBOEs, with the corresponding fluorescence lifetimes listed in Table 3. As indicated in Table 3, the fluorescent lifetimes of CCOBOE0 and CCOBOE1 are 2.04 and 2.00 ns respectively. This implies that CCOBOEs, upon excitation by a specific light source, exhibit advantages such as a rapid response and a high sensitivity, considering that the energy absorbed by the chromophore is rapidly transferred to the photocleavable groups, thereby facilitating the cleavage of the N-O bond. Furthermore, compared to CCOBOE0, BDEs of the N-O bonds in CCOBOE1 for the oxime ester groups connected to the carbazole and the coumarin moieties are significantly reduced, and determined as being $52.9 \text{ kcal}\cdot\text{mol}^{-1}$ and $50.7 \text{ kcal}\cdot\text{mol}^{-1}$, respectively. Consequently, enthalpies of the cleavage process of the N-O bond ($\Delta H_{\text{Cleavage } S1}$) exhibit markedly negative values of $-13.9 \text{ kcal}\cdot\text{mol}^{-1}$ and $-16.1 \text{ kcal}\cdot\text{mol}^{-1}$, respectively, which positively contribute to the easiness of the N-O bond cleavage and the decarboxylation reaction in CCOBOE1. Conversely, photocleavage from the triplet excited state is not favorable, E_T of CCOBOE1 being of $45.3 \text{ kcal}\cdot\text{mol}^{-1}$.

Table 3. N-O BDE, E_{S1} , E_T , $\Delta H_{\text{Cleavage } S1}$, $\Delta H_{\text{Cleavage } T1}$ and lifetimes of different CCOBOEs

CCOBOEs	N-O BDE (kcal.mol ⁻¹)	E_{S1} (kcal.mol ⁻¹)	$\Delta H_{\text{Cleavage } S1}$ (kcal.mol ⁻¹)	E_T (kcal.mol ⁻¹)	$\Delta H_{\text{Cleavage } T1}$ (kcal.mol ⁻¹)	Lifetime (ns)
CCOBOE0	63.6 ^a	66.8	-3.2 ^a	43.8	19.8 ^a	2.04
	62.1 ^b		-4.7 ^b		19.8 ^b	
CCOBOE1	52.9 ^a	66.8	-13.9 ^a	45.3	7.6 ^a	2.00
	50.7 ^b		-16.1 ^b		5.4 ^b	

a: oxime ester group connected to the carbazole group;

b: oxime ester group connected to the coumarin group.

FT-IR results were also utilized to confirm whether CCOBOE1 could undergo a decarboxylation reaction, resulting in the production of CO₂ during the photopolymerization. Figure 6 illustrates the infrared absorption spectra of the CCOBOE0/TMPTA and CCOBOE1/TMPTA systems at two different concentrations (5×10^{-6} mol.g⁻¹ and 2×10^{-5} mol.g⁻¹) after irradiation at 385, 405 and 450 nm with LEDs for 0, 30 and 60s. Analyses revealed the CO₂ peak to be detected at the three different wavelengths. Due to the lower content of photoinitiator in the 5×10^{-6} mol.g⁻¹ CCOBOE1/TMPTA system, the height of the CO₂ absorption peak is significantly lower compared to the 2×10^{-5} mol.g⁻¹ CCOBOE1/TMPTA system. Nevertheless, overall, these data positively support the proposed photolysis mechanism of CCOBOE1 upon light excitation.

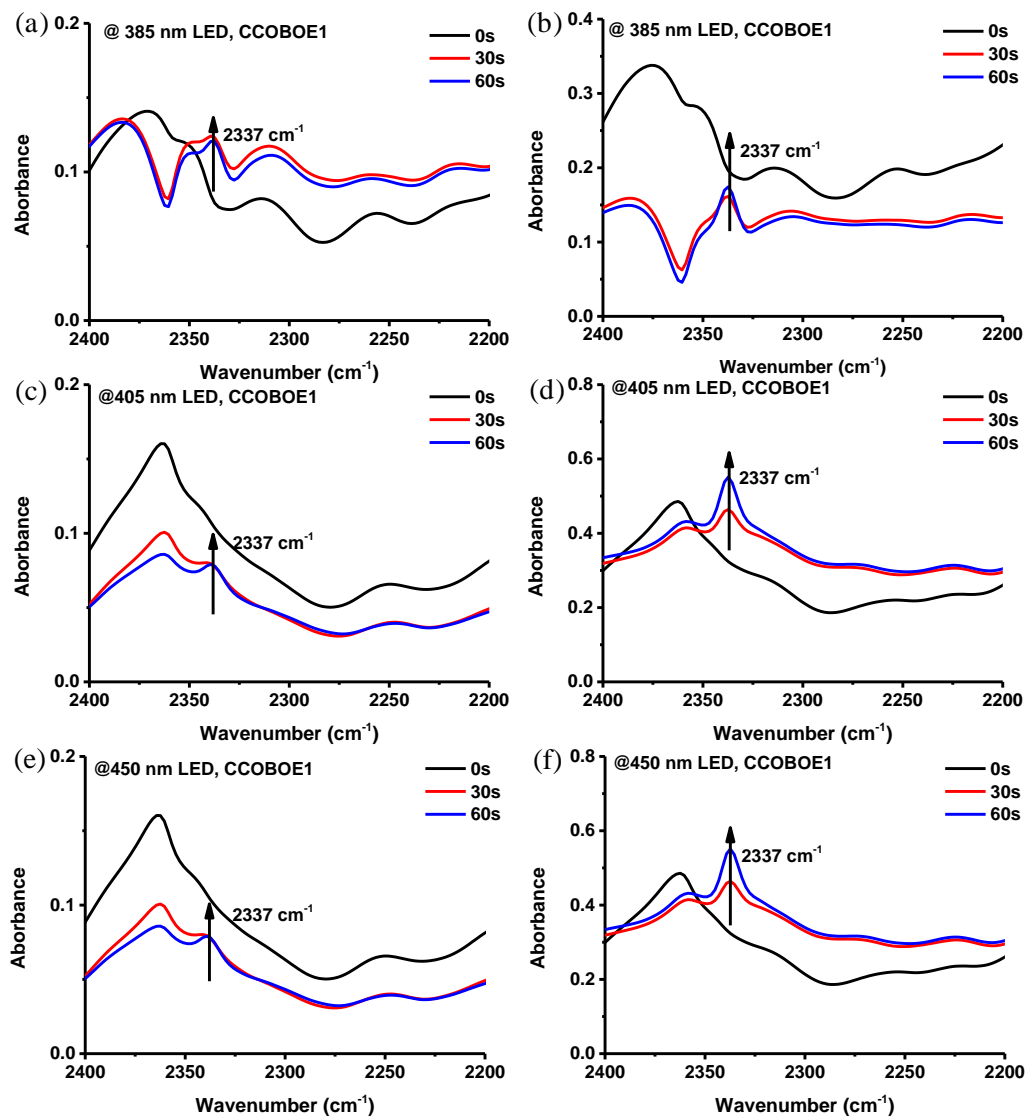
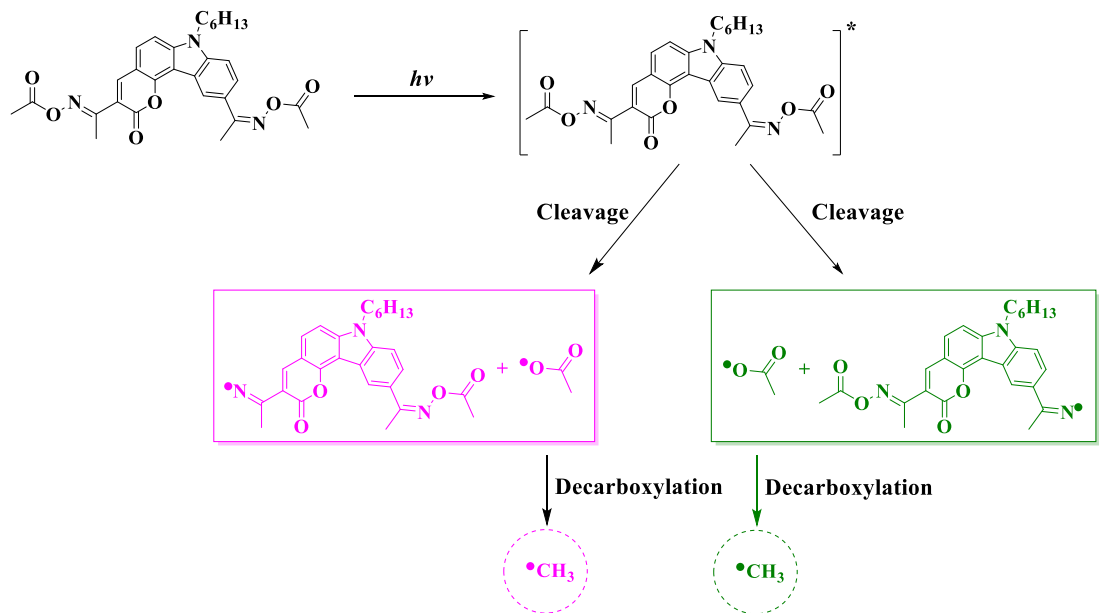


Figure 6. Infrared spectra of CCOBOE1 in TMPTA at $t = 0$, 30 and 60 s and the absorption intensity of CO_2 obtained from the CCOBOE1/TMPTA system respectively under 385 nm LED (a, b), 405 nm LED (c, d) and 450 nm (e, f). a, c, e, concentration is $5 \times 10^{-6} \text{ mol.g}^{-1}$; b, d, f concentration is $2 \times 10^{-5} \text{ mol.g}^{-1}$

2.6 Proposed chemical mechanism

Based on the experimental findings mentioned above, the mechanism for the generation of radicals from CCOBOE1 is proposed in Scheme 2. Upon excitation by light, the electrons within the CCOBOE1 molecule transition from the ground state to the excited state, absorbing energy. The unstable excited state transfers energy through intramolecular charge transfer, ultimately causing the low-energy N-O bond to undergo cleavage. This results in the formation of two moles of acyloxy radicals and one mole of carbazole-coumarin iminyl radicals. The unstable acyloxy radicals further decarboxylate, generating two moles of methyl radicals necessary for initiating the polymerization of acrylate monomers.

To further corroborate the proposed photolysis mechanism of CCOBOE1, ESR experiments were employed to capture radicals with unpaired electrons dissolved in *tert*-butylbenzene as the solvent. As depicted in Figure 7, after 15 s of irradiation with a 405 nm LED, no radicals were detected in the CCOBOE0/*tert*-butylbenzene solution. As expected, in the CCOBOE1/*tert*-butylbenzene solution, presence of acetoxy radicals was confirmed by calculating hyperfine coupling constants α_{H} and α_{N} , which were determined to be 1.8 G and 13.5 G respectively, and the presence of methyl radicals was evidenced by α_{H} and α_{N} values of 3.7 G and 14.6 G respectively.^[33-35] Therefore, the proposed photolysis mechanism of CCOBOE1 was validated by the ESR experiments.



Scheme 2. Suggested mechanism for CCOBOE1

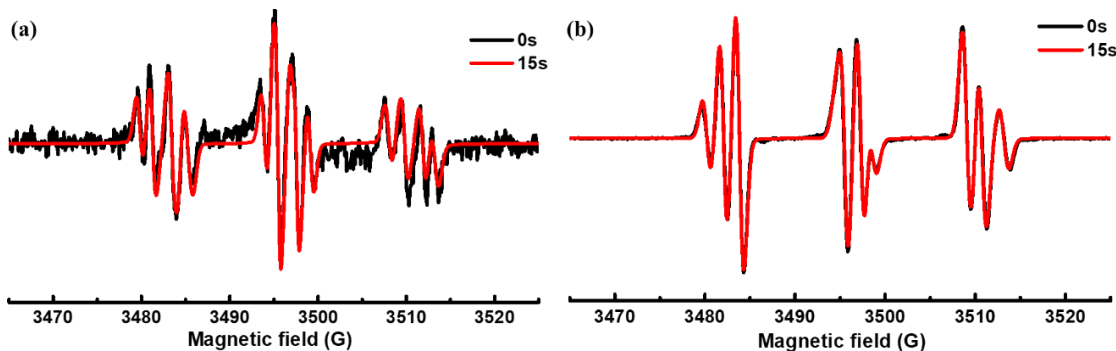


Figure 7. ESR-ST spectra of the PBN radical adducts of CCOBOE0 (a) and CCOBOE1 (b) under LED@405 nm irradiation in *tert*-butylbenzene

2.7 DLW and 3D printing

In order to assess the practical application of the CCOBOE1/TMPTA system in 3D printing, we conducted an evaluation focusing on the accuracy and the spatial resolution of the resulting 3D patterns. A concentration of 5×10^{-6} mol.g⁻¹ of CCOBOE1/TMPTA was selected for use in direct laser writing (DLW) and 3D printing to print the pre-determined patterns and object under 405 nm LED irradiation. As depicted in Figures 8 (a, b), despite the entire 3D printing process was conducted in an environment exposed to air, the "XYZ" pattern with a thickness of 963 μm and the 3D-printed object were successfully produced within 2 min and overnight respectively. Through numerical optical microscopy, it was observed that the printed pattern surface was

remarkably smooth, and the outlines of the three letters exhibited high accuracy and resolution. Additionally, as described in Figure 8 (c, d, e), the selected models were successfully fabricated via a 3D printer (Anycubic DLP Photon D2), exhibiting remarkably smooth surfaces and precise external as well as internal contours. This remarkable resolution can be confidently assigned to the efficient cleavage of CCOBOE1, which generates highly reactive methyl radicals when excited by light.

It is worth noting that when a higher concentration of 2×10^{-5} mol.g⁻¹ of the CCOBOE1/TMPTA system was utilized, the "XYZ" pattern shown in Figure 8 was not successfully printed. This may be related to the inability of the DLW light source to penetrate in depth the resin at high concentration of the CCOBOE1/TMPTA system. In conclusion, the CCOBOE1/TMPTA system proves to be highly suitable for industrial applications in laser manufacturing, showcasing excellent accuracy and resolution.

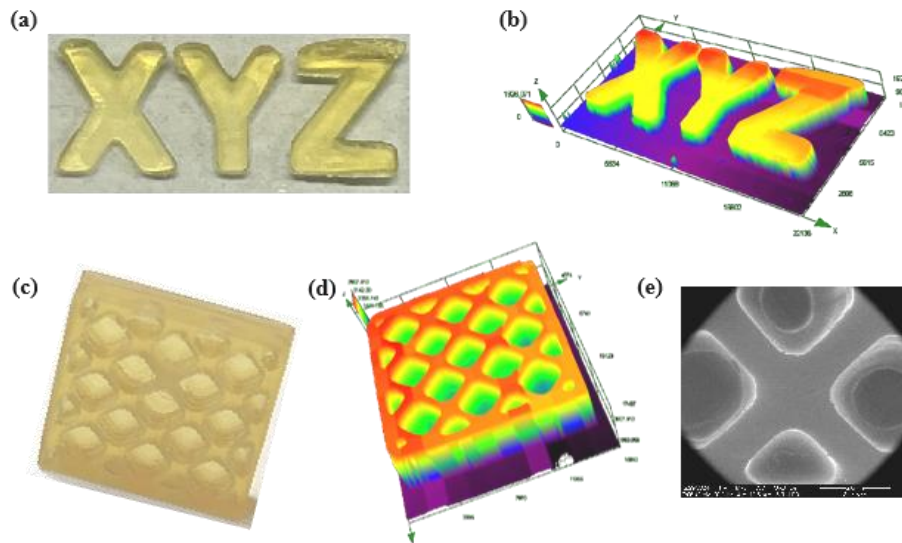


Figure 8. DLW printing patterns (a) and characterization by numerical optical microscopy (b); 3D printing object (c) and characterization by numerical optical microscopy (d) and SEM (e)

2.8 Thermal behavior polymerization

The thermal polymerization behavior of CCOBOEs (2×10^{-5} mol.g⁻¹) using TMPTA as the monomer was evaluated by Differential Scanning Calorimetry (DSC) measurements. The initial decomposition temperature (T_{initial}), maximum

decomposition temperature (T_{\max}), and FCs of CCOBOEs are presented in Table S1. As shown in Figure 9, CCOBOE0 exhibited an initial temperature for initiating TMPTA polymerization at 91 °C, with a T_{\max} of 218 °C. In comparison, CCOBOE1/TMPTA exhibited lower T_{initial} and T_{\max} , specifically 83 °C and 176 °C, respectively. This is attributed to the fact that CCOBOE1 which is an oxime ester is also prone to thermal cleavage, as indicated by its excellent thermal polymerization ability. Gratifyingly, CCOBOE1 achieved a FC of 65% during sustained heating, surpassing CCOBOE0 ($\text{FC}_{\text{CCOBOE}0} = 59\%$). This suggests that CCOBOE1 not only serves as a radical photoinitiator but also as a radical thermal initiator.

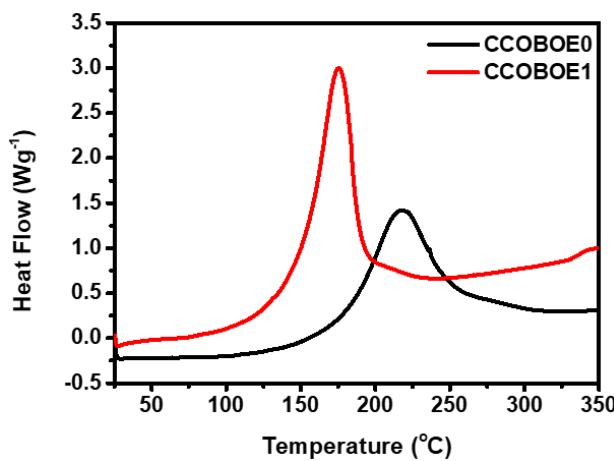


Figure 9. DSC curves of CCOBOE0/TMPTA, CCOBOE1/TMPTA systems

3. Conclusion

In this study, a novel carbazole-coumarin hybrid dye comprising two oxime ester groups was designed and successfully synthesized, and this bifunctional OXE is the first to be reported for this family of dyes. Influence of irradiation wavelength and the concentration of CCOBOEs on the photoinitiating efficiency of TMPTA was investigated. The optimal formulation (concentration and light source) was identified through free radical polymerization experiments. It has been demonstrated that the introduction of the *bis*-oxime ester, which can generate more active free radicals, indeed enhances the final conversion rate of acrylate monomer polymerization. Additionally, the photolysis mechanism of CCOBOE1 was proposed and validated through the detection of CO₂ absorption peaks, theoretical comparison of intramolecular bond

energies, and ESR experiments. Furthermore, the CCOBOEs/TMPTA system exhibited an excellent thermal polymerization efficiency. Meanwhile, the application of the CCOBOE1/TMPTA system in DLW and 3D printing demonstrated exceptionally high precision and clarity in pattern and object formation. In the future, the structural diversity of *bis*-oxime esters with photobleaching or water-soluble chromophores can be further enriched.

Acknowledgments

The authors thank the fundings provided by the ANR PhotoFlat and the Chinese Scholarship Council (CSC). The molecular modelling in this work was performed using HPC resources of the Mesocentre of the University of Strasbourg and the HPC resources from GENCI-IDRIS (Grant 2023-AD010812313R2/Jean_Zay).

Conflicts of interest

The manuscript was written through contributions of all authors. All authors have given their approval to the final version of the manuscript.

Notes

The authors declare no competing financial interest. The raw/processed data required to reproduce these findings can be furnished on demand.

References

- [1] J. Radebner, A. Eibel, M. Leypold, C. Gorsche, L. Schuh, R. Fischer, A. Torvisco, D. Neshchadin, R. Geier, N. Moszner, Tetraacylgermanes: highly efficient photoinitiators for visible-light-induced free-radical polymerization, *Angewandte Chemie International Edition* 56(11) (2017) pp. 3103-3107.
- [2] A. Jagtap, A. More, A review on self-initiated and photoinitiator-free system for photopolymerization, *Polymer Bulletin* 79(10) (2022) pp. 8057-8091.
- [3] S.M. Müller, S. Schlägl, T. Wiesner, M. Haas, T. Griesser, Recent advances in type I photoinitiators for visible light induced photopolymerization, *ChemPhotoChem* 6(11) (2022) p. e202200091.
- [4] F. Hammoud, A. Hijazi, M. Schmitt, F. Dumur, J. Lalevée, A review on recently proposed oxime ester photoinitiators, *European Polymer Journal* (2023) p. 111901.
- [5] F. Dumur, Recent advances on carbazole-based oxime esters as photoinitiators of polymerization, *European Polymer Journal* 175 (2022) p. 111330.
- [6] Z. Liu, F. Dumur, Recent advances on visible light Coumarin-based oxime esters as initiators of polymerization, *European Polymer Journal* (2022) p. 111449.
- [7] F. Hammoud, N. Giacoletto, G. Noirbent, B. Graff, A. Hijazi, M. Nechab, D. Gigmes, F. Dumur,

- J. Lalevée, Substituent effects on the photoinitiation ability of coumarin-based oxime-ester photoinitiators for free radical photopolymerization, *Materials Chemistry Frontiers* 5(24) (2021) pp. 8361-8370.
- [8] S. Liu, B. Graff, P. Xiao, F. Dumur, J. Lalevée, Nitro-Carbazole Based Oxime Esters as Dual Photo/Thermal Initiators for 3D Printing and Composite Preparation, *Macromolecular Rapid Communications* 42(15) (2021) p. 2100207.
- [9] Z.-H. Lee, F. Hammoud, A. Hijazi, B. Graff, J. Lalevée, Y.-C. Chen, Synthesis and free radical photopolymerization of triphenylamine-based oxime ester photoinitiators, *Polymer Chemistry* 12(9) (2021) pp. 1286-1297.
- [10] Z.H. Lee, T.L. Huang, F. Hammoud, C.C. Chen, A. Hijazi, B. Graff, J. Lalevée, Y.C. Chen, Effect of the Steric Hindrance and Branched Substituents on Visible Phenylamine Oxime Ester Photoinitiators: Photopolymerization Kinetics Investigation through Photo-DSC Experiments, *Photochemistry and Photobiology* 98(4) (2022) pp. 773-782.
- [11] J.B. Hsieh, S.C. Yen, F. Hammoud, J. Lalevée, Y.C. Chen, Effect of Terminal Alkyl Chains for Free Radical Photopolymerization Based on Triphenylamine Oxime Ester Visible-Light Absorbing Type I Photoinitiators, *ChemistrySelect* 8(30) (2023) p. e202301297.
- [12] Y.-H. Wu, A. Noon, F. Hammoud, T. Hamieh, J. Toufaily, B. Graff, J. Lalevée, Y.-C. Chen, Multibranched triarylamine end-capped oxime esters as visible-light absorbing type I photoinitiators for free radical photopolymerization, *Polymer Chemistry* 14(30) (2023) pp. 3421-3432.
- [13] Z.-H. Lee, S.-C. Yen, F. Hammoud, A. Hijazi, B. Graff, J. Lalevée, Y.-C. Chen, Naphthalene-Based Oxime Esters as Type I Photoinitiators for Free Radical Photopolymerization, *Polymers* 14(23) (2022) p. 5261.
- [14] W. Qiu, J. Zhu, K. Dietliker, Z. Li, Polymerizable Oxime Esters: An Efficient Photoinitiator with Low Migration Ability for 3D Printing to Fabricate Luminescent Devices, *ChemPhotoChem* 4(11) (2020) pp. 5296-5303.
- [15] W. Qiu, M. Li, Y. Yang, Z. Li, K. Dietliker, Cleavable coumarin-based oxime esters with terminal heterocyclic moieties: photobleachable initiators for deep photocuring under visible LED light irradiation, *Polymer Chemistry* 11(7) (2020) pp. 1356-1363.
- [16] C. Elian, N. Sanosa, N. Bogliotti, C. Herrero, D. Sampedro, D.-L. Versace, An anthraquinone-based oxime ester as a visible-light photoinitiator for 3D photoprinting applications, *Polymer Chemistry* 14(28) (2023) pp. 3262-3269.
- [17] W. Wang, M. Jin, H. Pan, D. Wan, Phenylthioether thiophene-based oxime esters as novel photoinitiators for free radical photopolymerization under LED irradiation wavelength exposure, *Progress in Organic Coatings* 151 (2021) p. 106019.
- [18] W. Wang, M. Jin, H. Pan, D. Wan, Remote effect of substituents on the properties of phenyl thienyl thioether-based oxime esters as LED-sensitive photoinitiators, *Dyes and Pigments* 192 (2021) p. 109435.
- [19] Y. Ding, S. Jiang, Y. Gao, J. Nie, H. Du, F. Sun, Photochromic Polymers Based on Fluorophenyl Oxime Ester Photoinitiators as Photoswitchable Molecules, *Macromolecules* 53(14) (2020) pp. 5701-5710.
- [20] S. Chen, M. Jin, J.-P. Malval, J. Fu, F. Morlet-Savary, H. Pan, D. Wan, Substituted stilbene-based oxime esters used as highly reactive wavelength-dependent photoinitiators for LED photopolymerization, *Polymer Chemistry* 10(48) (2019) pp. 6609-6621.

- [21] Y. Pang, S. Fan, Q. Wang, D. Oprych, A. Feilen, K. Reiner, D. Keil, Y.L. Slominsky, S. Popov, Y.J.A.C. Zou, NIR-Sensitized Activated Photoreaction between Cyanines and Oxime Esters: Free-Radical Photopolymerization, *Angewandte Chemie* 132(28) (2020) pp. 11537-11544.
- [22] S. Liu, N. Giacoletto, B. Graff, F. Morlet-Savary, M. Nechab, P. Xiao, F. Dumur, J. Lalevée, N-naphthalimide ester derivatives as Type I photoinitiators for LED photopolymerization, *Materials Today Chemistry* 26 (2022) p. 101137.
- [23] F. Hammoud, A. Pavlou, A. Petropoulos, B. Graff, M.G. Siskos, A. Hijazi, F. Morlet-Savary, F. Dumur, J. Lalevée, Naphthoquinone-based imidazolyl esters as blue-light-sensitive Type I photoinitiators, *Polymer Chemistry* 13(33) (2022) pp. 4817-4831.
- [24] T. Yu, Z. Zhu, Y. Bao, Y. Zhao, X. Liu, H. Zhang, Investigation of novel carbazole-functionalized coumarin derivatives as organic luminescent materials, *Dyes Pigments* 147 (2017) pp. 260-269.
- [25] N. Sekar, P.G. Umape, S.K. Lanke, Synthesis of novel carbazole fused coumarin derivatives and DFT approach to study their photophysical properties, *Journal of fluorescence* 24 (2014) pp. 1503-1518.
- [26] F. Dumur, Recent advances on carbazole-based photoinitiators of polymerization, *European Polymer Journal* 125 (2020) p. 109503.
- [27] F. Dumur, Recent advances on coumarin-based photoinitiators of polymerization, *European Polymer Journal* 163 (2022) p. 110962.
- [28] T. Yu, Z. Zhu, Y. Bao, Y. Zhao, X. Liu, H. Zhang, Investigation of novel carbazole-functionalized coumarin derivatives as organic luminescent materials, *Dyes and Pigments* 147 (2017) pp. 260-269.
- [29] M. Patel, N. Pandey, J. Timaniya, P. Parikh, A. Chauhan, N. Jain, K. Patel, Coumarin–carbazole based functionalized pyrazolines: Synthesis, characterization, anticancer investigation and molecular docking, *RSC advances* 11(44) (2021) pp. 27627-27644.
- [30] R. Zhou, X. Sun, R. Mhanna, J.-P. Malval, M. Jin, H. Pan, D. Wan, F. Morlet-Savary, H. Chaumeil, C. Joyeux, Wavelength-Dependent, Large-Amplitude Photoinitiating Reactivity within a Carbazole-Coumarin Fused Oxime Esters Series, *ACS Applied Polymer Materials* 2(5) (2020) pp. 2077-2085.
- [31] Y. Zhang, Z. Liu, T. Borjigin, B. Graff, F. Morlet-Savary, M. Schmitt, D. Gigmes, F. Dumur, J. Lalevée, Carbazole-fused coumarin based oxime esters (OXEs): efficient photoinitiators for sunlight driven free radical photopolymerization, *Green Chemistry* 25(17) (2023) pp. 6881-6891.
- [32] A. Kowalska, J. Sokolowski, K. Bociong, The photoinitiators used in resin based dental composite—a review and future perspectives, *Polymers* 13(3) (2021) p. 470.
- [33] S. Liu, N. Giacoletto, M. Schmitt, M. Nechab, B. Graff, F. Morlet-Savary, P. Xiao, F. Dumur, J.J.M. Lalevee, Effect of Decarboxylation on the Photoinitiation Behavior of Nitrocarbazole-Based Oxime Esters, *Macromolecules* 55(7) (2022) pp. 2475-2485.
- [34] Y. Zhang, B. Song, C. Dietlin, F. Morlet-Savary, M. Schmitt, F. Dumur, J. Lalevée, Naphthoquinone-Based Oxime Esters for Free Radical Photopolymerization under Sunlight or a Blue Light-Emitting Diode, *Industrial & Engineering Chemistry Research* (2024).
- [35] L.D. Haire, P.H. Krygsman, E.G. Janzen, U.M. Oehler, Correlation of radical structure with EPR spin adduct parameters: utility of the proton, carbon-13, and nitrogen-14 hyperfine splitting constants of aminoxy adducts of PBN-nitronyl-13C for three-parameter scatter plots, *The Journal of Organic Chemistry* 53(19) (1988) pp. 4535-4542.

